Entanglement signatures for the dimerization transition in the Majumdar-Ghosh model

M. S. Ramkarthik,[1,*] V. Ravi Chandra,[2,†] and Arul Lakshminarayan[1,‡]

[1]*Department of Physics, Indian Institute of Technology Madras, Chennai, 600036, India*

[2]*School of Physical Sciences, National Institute of Science Education and Research, Institute of Physics Campus, P.O. Sainik School,*
Bhubaneswar, 751005, India

The transition from a gapless liquid to a gapped dimerized ground state that occurs in the frustrated antiferromagnetic Majumdar-Ghosh (or $J_1 - J_2$ Heisenberg) model is revisited from the point of view of entanglement. We study the evolution of entanglement spectra, a "projected subspace" block entropy, and concurrence in the Schmidt vectors through the transition. The standard tool of Schmidt decomposition along with the existence of the unique Majumdar-Ghosh (MG) point where the ground states are degenerate and known exactly suggest the projection into two orthogonal subspaces that is useful even away from this point. Of these, one is a dominant five-dimensional subspace containing the complete state at the MG point and the other contributes marginally, albeit with increasing weight as the number of spins is increased. We find that the marginally contributing subspace has a minimum von Neumann entropy in the vicinity of the dimerization transition. Entanglement content between pairs of spins in the Schmidt vectors, studied via concurrence, shows that those belonging to the dominant five-dimensional subspace display a clear progress towards dimerization as the MG point is approached. In contrast, study of the Schmidt vectors in the marginally contributing subspace, as well as in the projection of the ground state in this space, display pair concurrence which decreases on both sublattices as the MG point is approached. The robustness of these observations indicate their possible usefulness in the study of models that have similar transitions, and have hitherto been difficult to study using standard entanglement signatures.

I. INTRODUCTION

Entanglement in many-body systems has been extensively studied recently [1–6] ever since the remarkable properties of quantum entanglement have come to be understood, especially through its various uses in quantum information processing [7–11]. Quantum phase transitions [12] which occur at zero temperature as some external parameter is changed has been particularly addressed with the help of entanglement [13–16]. The Ising-model critical point, for example, has been shown to have an entropy of entanglement that scales logarithmically ($\sim \ln L$) with the length L of the spin chain, while away from criticality it is independent of L [17–19]. While many condensed matter systems have been studied with the help of such a "block" entanglement entropy [17,19–25], it seems more natural to consider measures of two-body entanglement like concurrence [26] in contexts where dimerization occurs [27–30]. One of the well-studied Hamiltonians in this context is the Majumdar-Ghosh (MG) or the $J_1 - J_2$ Heisenberg model [31,32]. This model has a well-known transition from a gapless critical phase to a gapped phase with short-range correlations and dimer order [33,34]. Earlier studies with this model from the entanglement perspective have employed scaling behaviors of the von Neumann entropy of contiguous blocks of spins, the valence-bond entanglement entropy [15,35,36], and other measures of multipartite entanglement [37] to study this transition.

Direct signatures of the dimerization transition in this model using two-spin entanglement measures such as concurrence have been elusive. In the $J_1 - J_2$ model the antiferromagnetic nearest-neighbor Heisenberg chain is augmented with a next-nearest-neighbor Heisenberg interaction which is also antiferromagnetic [31,32,38]. The interest in this has been considerable since Majumdar and Ghosh proposed this as a model with an exactly solvable ground state that shows dimerization at $J_2/J_1 = 1/2$; the so-called MG point. The Hamiltonian is

$$H = J_1 \sum_{i=1}^{N} \vec{\sigma}_i \cdot \vec{\sigma}_{i+1} + J_2 \sum_{i=1}^{N} \vec{\sigma}_i \cdot \vec{\sigma}_{i+2}, \qquad (1)$$

with J_1, $J_2 > 0$. The particles are spin-$\frac{1}{2}$ and $\vec{\sigma}_i$ are the Pauli matrices. Periodic boundary conditions are assumed so that $\vec{\sigma}_{N+1} = \vec{\sigma}_1$ and $\vec{\sigma}_{N+2} = \vec{\sigma}_2$. At the MG point the ground state is doubly degenerate and the ground-state manifold is spanned by two states $|R_N\rangle$ and $|L_N\rangle$, where

$$\begin{aligned} |R_N\rangle &= (1\,2)(3\,4)\cdots(N-1\,N), \\ |L_N\rangle &= (2\,3)(4\,5)\cdots(N\,1). \end{aligned} \qquad (2)$$

Here, for example, (1 2) refers to the singlet state $\frac{1}{\sqrt{2}}(|01\rangle - |10\rangle)$ of spins 1 and 2, and $|0\rangle$ and $|1\rangle$ are eigenstates of σ_z with eigenvalues 1 and -1, respectively. Thus at the MG point the degenerate ground states can be considered to have maximal nearest-neighbor entanglements as the entanglement of a singlet is the maximum possible between two spin-$\frac{1}{2}$ particles. Thus it would seem natural that entanglement between spins is enhanced at a transition from a spin-liquid to a dimerized phase [33,34], a transition which occurs when $J_2/J_1 \approx 0.24\ldots$. While a fair amount of literature

---
*ramkarthik@physics.iitm.ac.in
†ravi@niser.ac.in
‡arul@physics.iitm.ac.in

already addresses this [15,37,39], the present paper revisits the issues from the point of view of analysis of entanglement spectra at finite lattice sizes, a nonstandard block entropy, and concurrences in the Schmidt vectors of the reduced density matrices. We expect this to be of interest in larger classes of problems where the possibility of transitions from spin liquid to dimer order need to be investigated.

Few earlier works concentrate more on the MG point at $J_2/J_1 = 1/2$. For example, some concurrence-based quantities were studied as potential indicators of the level crossing and transition at this point in Ref. [15]. The pairwise concurrence between the nearest-neighbor sites (NN) and that of the next-nearest-neighbor sites (NNN) was studied both at finite temperatures and for the ground state in Ref. [27], where it was found that the NN concurrence decreases while the NNN concurrence increases with increasing J_2 and that, at the MG point, these quantities have singularities, which originate clearly due to the crossing. It was also found in Ref. [36] that it is the NNN entanglement entropy, rather than concurrence, that has a maximum at the MG point.

As mentioned earlier, attention in the present work is centered in the range $0 \leqslant J_2/J_1 \leqslant 1/2$ and especially the dimerization occurring therein. The strategy, though, is to focus on the fact that this is one of the rare systems where at least at one point in the phase diagram (namely, the MG point) the ground state can be solved for exactly and has a form simple enough to enable the evaluation of the entanglement spectrum analytically. The nature of the entanglement spectrum at this point suggests a separation of the state into two orthogonal components with supports in what one may call a "MG" and a "non-MG" subspace. At the MG point, the MG subspace *solely* contributes towards the construction of the ground states, hence the terminology. The MG subspace is only five dimensional and in the range $0 \leqslant J_2/J_1 \leqslant 1/2$ seems dominant at least for small system sizes. In fact, the competition between this subspace and its complement seems to be crucial for the emergence of a dimer order. For later convenience the non-MG subspace is denoted as $\overline{MG}$. However, these subspaces are not unique in a way that is elaborated in the next section.

It is found that a suitably defined entanglement corresponding to the $\overline{MG}$ component of the wave function has a minimum in the vicinity of the dimerization transition. Thus, while there do not seem to be simple signatures (except for scaling with L) in either the entanglement entropy of the state [36], or its dominant part (namely, the MG component), the typically small $\overline{MG}$ components apparently carry information that may signal the transition. The separation of the entanglement spectrum into these two components also allows for a detailed study of the entanglement of the *eigenvectors* of the reduced density matrices. While much attention has concentrated on the entanglement spectrum per se, it is but natural that the eigenvectors have significant information in them. The entanglement in these Schmidt vectors is studied, especially the concurrence between nearest neighbors. It is observed that, for vectors corresponding to the MG component, a clear dimerization happens, with alternate pairs of nearest-neighbor entanglements either increasing to the maximum value as the MG point is approached, or vanish in the vicinity of the dimerization transition.

II. EIGENVALUE SPECTRUM OF GROUND STATE OF MAJUMDAR-GHOSH MODEL

First, we seek a separation of the ground state of the MG Hamiltonian, say $|\Psi(J_2)\rangle$ ($J_1 = 1$ from now on), into two distinct orthogonal states with the properties described below. Thus,

$$|\Psi(J_2)\rangle = \alpha(J_2)|\psi_{MG}(J_2)\rangle + \beta(J_2)|\psi_{\overline{MG}}(J_2)\rangle, \qquad (3)$$

where $|\psi_{MG}(J_2)\rangle$ approaches a superposition of $|R_N\rangle$ and $|L_N\rangle$ as $J_2 \to 1/2$, and $\alpha(J_2) \to 1$, $\beta(J_2) \to 0$ in the same limit. The state $|\psi_{\overline{MG}}(J_2)\rangle$ is orthogonal to this and will play a rather important role here. This non-MG part forms a small fraction of the whole state, at least for small N (e.g., 3% for $N = 16$). With increasing number of spins, though, this component grows and the detailed manner in which this happens as a function of J_2 is interesting and may hold information about the dimerization. However, by definition this component decreases to zero at the MG point ($J_2 = 1/2$) for *all* N. Such a separation is possible but is potentially nonunique, as demonstrated further below. Throughout this paper the number of spins is an even number, and there are two main subclasses: $N/2$ even and $N/2$ odd, which are simply referred to as "even" and "odd" cases. Also from the point of view of symmetry, the translation symmetry is broken in the projected MG and $\overline{MG}$ parts for all J_2.

One would especially like to treat the interval $0 \leqslant J_2 < 1/2$, which contains the point where there is a gapless-to-gapped transition. When $J_2 = 0$ the ground state (and indeed any excited state) is solvable via the Bethe ansatz [40]; however, the explicit forms are unwieldy and difficult to analyze in detail. Thus a rather "complex" antiferromagnetic ground state at $J_2 = 0$ evolves to a rather simple dimerized state at $J_2 = 1/2$. That a part of the ground state can be identified for all J_2 in the interval $[0, 1/2)$ that evolves to the dimers at the MG point is not necessarily obvious and is elucidated in this paper.

That this is possible is strongly suggested from a study of the Schmidt decomposition of the ground state. Let N spins in the chain be split into two parts (say A and B) of contiguous spins having N_A and N_B particles each. This paper will concentrate on the cases when N_A and N_B are even numbers as well. This ensures that the subsystems under consideration are of the same parity (number of spins odd or even) as the original chain. The Schmidt decomposition in terms of vectors from these two halves reads

$$|\Psi(J_2)\rangle = \sum_{j=1}^{2^{N_A}} \sqrt{\lambda_j(J_2)}|\phi_j(J_2)\rangle_A |\phi_j(J_2)\rangle_B. \qquad (4)$$

Here, $\lambda_j(J_2)$ are the eigenvalues of the reduced density matrix (RDM)

$$\rho_{N_A}(J_2) = \text{tr}_B\left[|\Psi(J_2)\rangle\langle\Psi(J_2)|\right],$$

and $|\phi_j(J_2)\rangle_A$ are the corresponding eigenvectors. The eigenvalues $\lambda_j(J_2)$ are also dependent on the partition size N_A, but this is not explicitly indicated. The von Neumann entropy $S_{N_A}(J_2) = -\sum_{j=1}^{2^{N_A}} \lambda_j(J_2) \log_2[\lambda_j(J_2)]$ is a measure of the
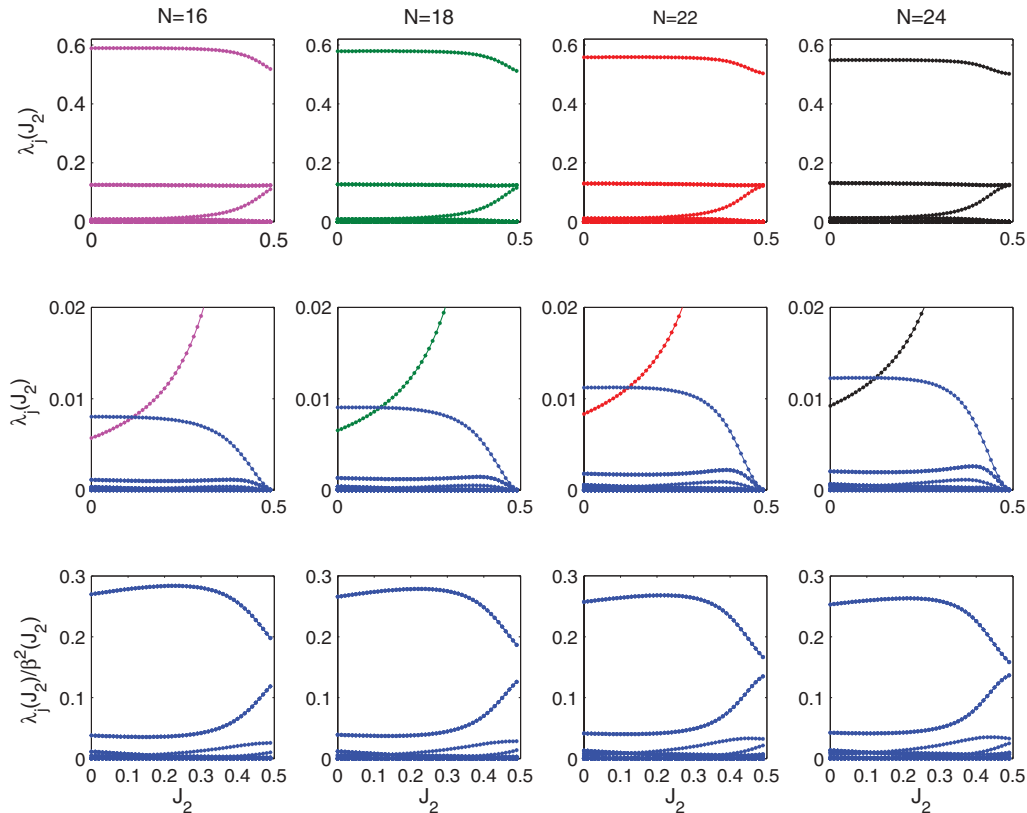
FIG. 1. (Color online) Eigenvalues of RDM $\rho_{N_A}(J_2)$ for $N = 16, 24$ (corresponding to $N_A = N/2$) and $N = 18$, $N = 22$ (corresponding to $N_A = N/2 - 1$). In the top row, the 50 largest eigenvalues are plotted. Prominently seen are the five "dimer" or MG subspace eigenvalues, a large eigenvalue around 0.6, the almost constant triplet around 0.1, and the small but rising eigenvalue that becomes important around the dimerization transition. The middle row shows the same as the top, but with the y axis magnified, showing the $\overline{MG}$ triplet eigenvalue (in one color) that crosses the rising singlet eigenvalue of the MG subspace (in a different color). The bottom row shows the $\overline{MG}$ eigenvalues rescaled so that their sum is unity. The largest 50 eigenvalues are shown.

entanglement between parts A and B. There have been several works that study the so-called entanglement spectrum [41–43] which is defined as $\{-\ln(\lambda_j),\ j = 1, 2, \ldots\}$ in many systems; such a spectrum naturally containing much more information than just the entropy. For most of this paper, unless otherwise mentioned, $N_A = N/2$ for the even case and $N_A = N/2 - 1$ for the odd case. It must be noted that only for the entanglement spectrum do we take the logarithm to the base e and for all other measures of entropy the logarithm is taken with respect to base 2. All of the numerical results in this paper are obtained from exact diagonalizations.

Figure 1 (top row) shows the eigenvalues of the RDM, where the principal eigenvalues corresponding to the MG subspace are seen clearly. The largest eigenvalue decreases as the MG point is approached from the Heisenberg. The second-largest eigenvalue actually consists of a triplet that is almost a constant as J_2 varies in $[0, 1/2]$. The smallest of the eigenvalues that is clearly visible in this figure increases as the MG point is approached and indeed seems to become significant in the vicinity of the dimerization transition. It is shown below that, at the MG point, this eigenvalue is coupled with the largest one. As $N \rightarrow \infty$, it approaches the value 1/8. The Schmidt vectors (pure states of $N/2$ particles) corresponding to these five eigenvalues along with identical

vectors from the remaining $N/2$ particles form the N-particle MG subspace.

Figure 1 (middle row) shows the intersection of the largest eigenvalue in $\overline{MG}$ (which is triply degenerate and shown using one color) with the rising eigenvalues of the dimer MG sector (shown using a different color). This is a robust feature for all N and an even number of spins in the subspaces. More of the eigenvalues corresponding to the $\overline{MG}$ subspace are seen in the bottom row which shows the rescaled eigenvalues in this sector. In the rescaled figure which shows only the $\overline{MG}$ eigenvalues, the most prominent ones are again few and the two that are shown correspond to a pair of triplets that seem to be coupled strongly.

Figure 2 shows the entanglement spectrum, defined as $-\ln(\lambda_j)$, plotted against J_2. This figure now highlights the small eigenvalues in the $\overline{MG}$ subspace and a clear separation is seen as those belonging to the MG subspace now decrease as the MG point is approached. There are several sharp peaks that are seen in these figures and their density increases with N. These signal eigenvalues of the RDM that either go exactly to zero or come very close to it (it is sometimes difficult to tell with given the numerical resolution in J_2) and interestingly resume their career immediately thereafter.
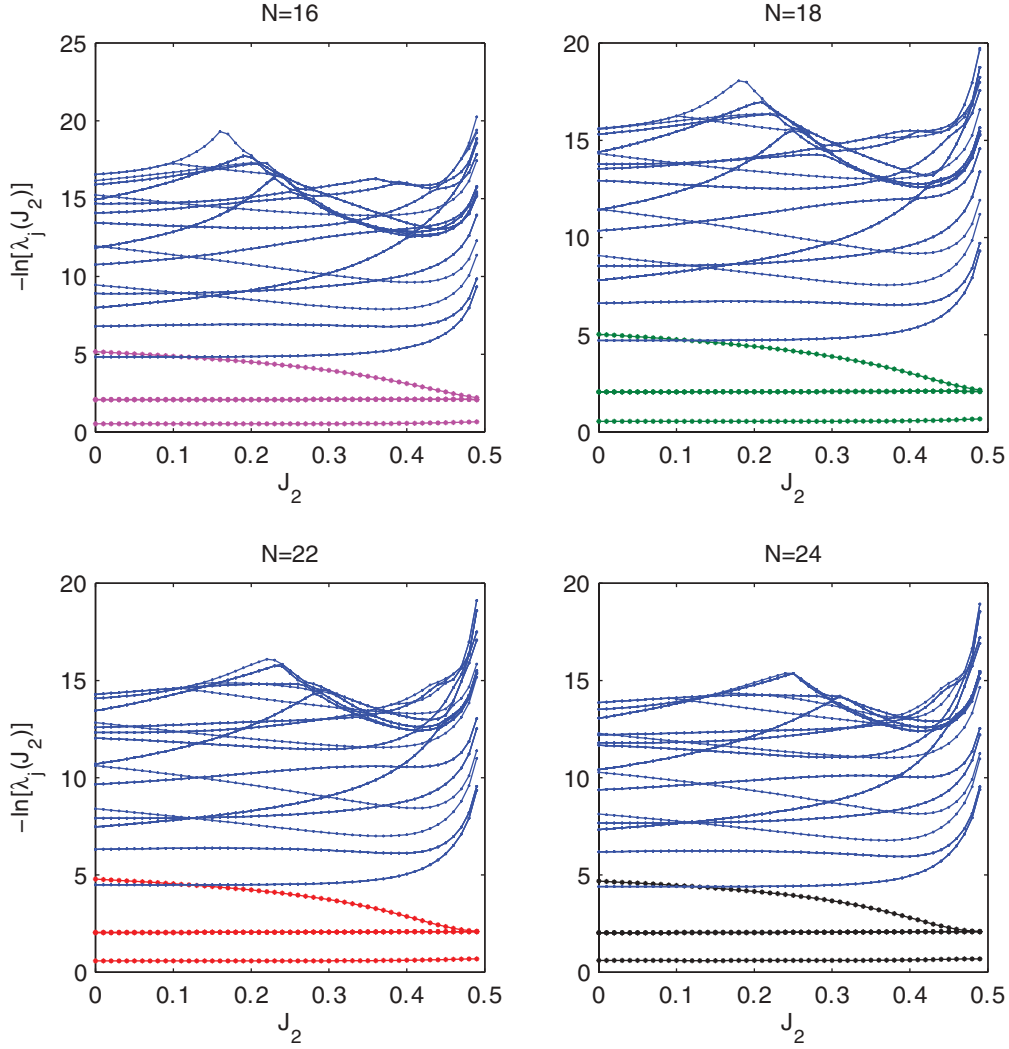
FIG. 2. (Color online) Entanglement spectrum that shows $\overline{MG}$ as excited states (50 of the largest density matrix eigenvalues are plotted). The separation of the MG and $\overline{MG}$ eigenvalues is seen clearly here, and the proliferating number of eigenvalues that vanish at isolated points along J_2 are seen as sharp peaks.

It is then quite apparent that there are only few dominant eigenvalues of the density matrix, even away from the MG point. That these are actually those that produce the dimer is made clear by studying the entanglement spectrum of a superposition of the dimers. Towards this end consider the state

$$|\Psi_{MG}\rangle = \alpha_1 |R_N\rangle + \alpha_2 |L_N\rangle, \tag{5}$$

where $|R_N\rangle$ and $|L_N\rangle$ are as defined in Eq. (2), and α_1 and α_2 are real. It is the simplest type of "valence-bond state," which is a superposition of dimerized states [44]. While in general such VBS states have been quite extensively studied, including from the point of view of entanglement [20,21,45–47] to our knowledge a detailed analysis of the simple state in $|\Psi_{MG}\rangle$ at finite N and arbitrary partition sizes has not been reported.

We begin here by evaluating the required RDMs. Let $N_A = 2k$ be the number of particles in the subsystem A (k is any appropriate integer > 1) whose density matrix is given by

(details are relegated to the Appendix)

$$
\begin{aligned}
\rho_A^{MG} &= \text{tr}_B \left(|\Psi_{MG}\rangle\langle\Psi_{MG}| \right) \\
&= \alpha_1^2 |R_{2k}\rangle\langle R_{2k}| + \alpha_2^2 \left[\frac{I_1}{2} \otimes |L_{2k-2}\rangle\langle L_{2k-2}| \otimes \frac{I_{2k}}{2} \right] \\
&\quad + \frac{\alpha_1\alpha_2}{2^{(N-2k)/2}} (-1)^{(N-2k)/2} \left[|R_{2k}\rangle\langle L_{2k}| + |L_{2k}\rangle\langle R_{2k}| \right],
\end{aligned}
\tag{6}
$$

where $|R_{2k}\rangle = (1\,2)\cdots(2k-1\,2k)$ and $|L_{2k-2}\rangle = (2\,3)\cdots(2k-2\,2k-1)$ while $|L_{2k}\rangle = |L_{2k-2}\rangle(2k\,1)$ are dimers of part A; $|L_{2k-2}\rangle$ does not contain the singlet between the first and the "last" $(2k)$ spin of part A. Because the inner product $\langle R_K | L_K \rangle = (-1)^{K/2}/2^{K/2-1}$, it is readily verified that $\text{tr}(\rho_A^{MG}) = \alpha_1^2 + \alpha_2^2 + 2\alpha_1\alpha_2\langle R_N | L_N \rangle = \langle \Psi_{MG} | \Psi_{MG} \rangle$. Thus, if α_1 and α_2 are taken such that $|\Psi_{MG}\rangle$ is normalized, the trace of the RDM ρ_A^{MG} is indeed 1.

To find the spectrum of ρ_A^{MG}, it is useful to express the identity operator in the space of spins 1 and $2k$, $I_1 \otimes I_{2k}$,

in terms of the complete set of corresponding Bell-state projectors. This results in

$$
\rho_A^{MG} = \alpha_1^2 |R_{2k}\rangle\langle R_{2k}| + \frac{\alpha_2^2}{4} |L_{2k}\rangle\langle L_{2k}| + \frac{\alpha_2^2}{4}\left(\sum_{l=1}^{3} |L_{2k}^l\rangle\langle L_{2k}^l|\right)
$$
$$
+ \frac{\alpha_1\alpha_2}{2^{(N-2k)/2}}(-1)^{(N-2k)/2}\left(|R_{2k}\rangle\langle L_{2k}| + |L_{2k}\rangle\langle R_{2k}|\right).
$$
(7)

Here, $|L_{2k}^l\rangle$ are $|L_{2k-2}\rangle \otimes |\phi_b^l\rangle_{2k,1}$, where $|\phi_b^1\rangle = (|01\rangle + |10\rangle)/\sqrt{2}$, $|\phi_b^2\rangle = (|00\rangle + |11\rangle)/\sqrt{2}$, and $|\phi_b^3\rangle = (|00\rangle - |11\rangle)/\sqrt{2}$ are three Bell states, the remaining one being the singlet that along with $|L_{2k-2}\rangle$ results in $|L_{2k}\rangle$. These Bell-state augmented dimers are quite easily seen to satisfy $\langle R_{2k}|L_{2k}^l\rangle = \langle L_{2k}|L_{2k}^l\rangle = 0$ for $l = 1, 2, 3$. Thus, $|L_{2k}^l\rangle$ are three degenerate eigenstates of ρ_A^{MG} with eigenvalues $\lambda_2^{MG} = \lambda_3^{MG} = \lambda_4^{MG} = \alpha_2^2/4$. Two other eigenstates are linear combinations of the nonorthogonal states $|R_{2k}\rangle$ and $|L_{2k}\rangle$, and the resultant eigenvalues are

$$
\lambda_{1,5}^{MG} = \frac{1}{2}\left[\left(\langle\Psi_{MG}|\Psi_{MG}\rangle - \frac{3\alpha_2^2}{4}\right) \pm \sqrt{\left(\langle\Psi_{MG}|\Psi_{MG}\rangle - \frac{3\alpha_2^2}{4}\right)^2 - \left(1 - \frac{4}{2^{2k}}\right)\left(1 - \frac{4}{2^{N-2k}}\right)\alpha_1^2\alpha_2^2}\right].
$$
(8)

These five eigenvalues of the $2k$-particle $(k > 1)$ RDM are the only nonzero ones, and it is easily verified that they add up to the trace of the RDM. If the initial dimer state is normalized they add to unity. They are ordered according to their typical magnitude, especially when $\alpha_1^2 = \alpha_2^2 = 1/2$, with λ_1^{MG} being the largest and λ_5^{MG} being the smallest eigenvalue. When $N = \infty$ and $\alpha_1^2 = \alpha_2^2 = 1/2$, the eigenvalues are, as indicated earlier, $(1/2, 1/8, 1/8, 1/8, 1/8)$ and the entropy or entanglement is 2 ebits. For finite N the entropy is smaller; for example, when $N = 8$ and $2k = 4$, taking the normalized state $|\Psi_{MG}\rangle$ with $\alpha_1 = \alpha_2 = 2/3$ leads to $\lambda_2^{MG} = \lambda_3^{MG} = \lambda_4^{MG} = 1/9$ as the eigenvalues for the degenerate triplet of states and the other two are $\lambda_1^{MG} = (2 + \sqrt{3})/6 \approx 0.622$ and $\lambda_5^{MG} = (2 - \sqrt{3})/6 \approx 0.044$, while the entanglement is ≈ 1.683 ebits. To take an example of an odd case, let $N = 10$ and $2k = 4$. The normalized state that has momentum π may be taken as $|\psi_{MG}\rangle = \sqrt{8/17}(|R_{10}\rangle - |L_{10}\rangle)$. Thus, with $\alpha_1 = -\alpha_2 = \sqrt{8/17}$, the above gives $\lambda_{2,3,4}^{MG} = 2/17 \approx 0.117$ and $\lambda_1^{MG} = (11 + 2\sqrt{19})/34 \approx 0.579$ and $\lambda_5^{MG} = (11 - 2\sqrt{19})/34 \approx 0.067$. This may be compared with the eigenvalues of the RDM near the MG point. For example, for $N = 10$ and $2k = 4$ when $J_2 = 0.4975$, the triplets in the dimerized part have eigenvalues of 0.1175, while the large eigenvalue and the smallest one in this part are 0.582 and 0.065, which indeed compare well with the numbers derived above.

Thus the "entanglement spectrum" at the MG point consists of only five levels. The fact that the ground state of the MG model for $0 \leqslant J_2 < 1/2$ does not undergo any crossings [15] indicates a certain robustness that will be reflected in the entanglement spectrum as well. As evidenced also by results shown in Figs. 1 and 2, indeed a five-dimensional subspace dominates the entanglement spectrum and evolves to the one derived above when $J_2 \to 1/2$. Thus Eq. (4) may be split into two parts with $|\Psi(J_2)\rangle = \sum_{j=1}^{5}\sqrt{\lambda_j(J_2)}|\phi_j(J_2)\rangle_A|\phi_j(J_2)\rangle_B + \sum_{j=6}^{2^{N_A}}\sqrt{\lambda_j(J_2)}|\phi_j(J_2)\rangle_A|\phi_j(J_2)\rangle_B$, which is the separation that is alluded to in Eq. (3). Thus $|\psi_{MG}(J_2)\rangle$ is in the five-dimensional "dimer" MG subspace that dominates the state, while $|\psi_{\overline{MG}}(J_2)\rangle$ belongs to the $(2^{N_A} - 5)$-dimensional subspace which constitutes the rest. The eigenvalues $\lambda_i(J_2)$ for $1 \leqslant i \leqslant 5$ are *defined* as those that evolve to λ_i^{MG} at the MG

point $J_2 = 1/2$. Thus it follows that

$$
\alpha^2(J_2) = \sum_{j=1}^{5}\lambda_j(J_2),
$$
$$
\beta^2(J_2) = \sum_{j=6}^{2^{N_A}}\lambda_j(J_2) = 1 - \alpha^2(J_2),
$$
$$
|\psi_{MG}(J_2)\rangle = \sum_{j=1}^{5}\sqrt{\frac{\lambda_j(J_2)}{\alpha^2(J_2)}}|\phi_j(J_2)\rangle_A|\phi_j(J_2)\rangle_B,
$$
$$
|\psi_{\overline{MG}}(J_2)\rangle = \sum_{j=6}^{2^{N_A}}\sqrt{\frac{\lambda_j(J_2)}{\beta^2(J_2)}}|\phi_j(J_2)\rangle_A|\phi_j(J_2)\rangle_B. \quad (9)
$$

The identification of the eigenvalues belonging to $\overline{MG}$ is complicated slightly by the fact that the largest eigenvalue in this set crosses the eigenvalue that becomes λ_5^{MG} of Eq. (8). Indeed, this "rising" eigenvalue in the dimer subspace is coupled to the largest eigenvalue state and its dominance in the spectrum seems correlated with the dimerization process.

It is important to note that the identification of the N-particle pure states $|\psi_{MG}(J_2)\rangle$ and $|\psi_{\overline{MG}}(J_2)\rangle$ from the Schmidt vectors is *dependent* on the partition sizes N_A and N_B and thus usage of terms such as MG and $\overline{MG}$ subspaces is predicated upon a definite partition dependence, usually the symmetric one, corresponding to $N_A = N_B$.

Following the above considerations, one may find three entanglements between N_A contiguous spins and the rest:

$$
S(J_2) = -\sum_{i=1}^{2^{N_A}}\lambda_i(J_2)\log_2[\lambda_i(J_2)],
$$
$$
S_{MG}(J_2) = -\sum_{i=1}^{5}\frac{\lambda_i(J_2)}{\alpha^2(J_2)}\log_2\left(\frac{\lambda_i(J_2)}{\alpha^2(J_2)}\right), \quad (10)
$$
$$
S_{\overline{MG}}(J_2) = -\sum_{i=6}^{2^{N_A}}\frac{\lambda_i(J_2)}{\beta^2(J_2)}\log_2\left(\frac{\lambda_i(J_2)}{\beta^2(J_2)}\right),
$$

whose interpretations as the entanglements in the ground state $[|\Psi(J_2)\rangle]$ and separately in the MG and $\overline{MG}$ parts $[|\psi_{MG}(J_2)\rangle$ and $|\psi_{\overline{MG}}(J_2)\rangle]$ of the ground state, respectively,
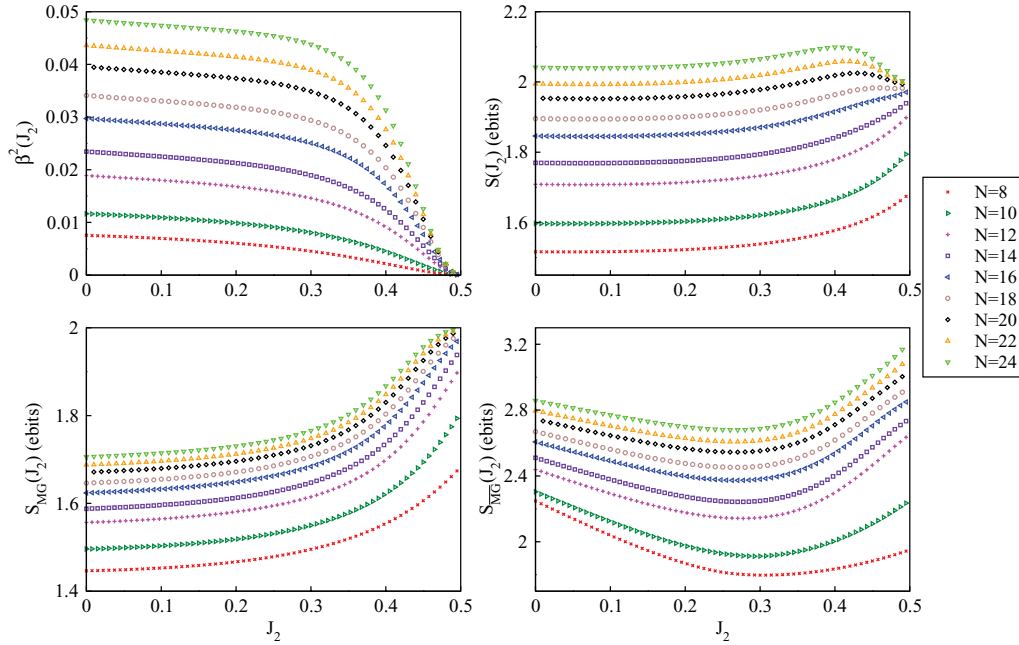
FIG. 3. (Color online) Sum of eigenvalues corresponding to $\overline{MG}$ subspace, $\beta^2(J_2)$, is shown on top-left plot for various values of number of spins N from $N = 8$ to $N = 24$ in steps of two, while the top-right plot shows the entanglement of N_A spins with the rest [the entropy $S(J_2)$] in the complete ground state. The bottom-left plot shows the entanglement of the projection in the MG subspace [the entropy $S_{MG}(J_2)$]. The entropy $S_{\overline{MG}}(J_2)$, which is the entanglement of the projection in the $\overline{MG}$ subspace as defined in Eq. (10), is shown in the bottom-right plot. $N_A = N/2$ for the even case and $N/2 - 1$ for the odd case.

is straightforward. The behaviors of $\beta^2(J_2)$ and $S(J_2)$ are shown respectively in the top-left and top-right plots of Fig. 3, while the bottom-left plot of Fig. 3 shows $S_{MG}(J_2)$, which is the entanglement in the MG subspace projection. The bottom-right plot shows $S_{\overline{MG}}(J_2)$. In these figures, for even cases ($N/2$ is even), $N_A = N/2$, while in the odd case $N_A = N/2 - 1$. It is interesting that while the entropies $S(J_2)$ and S_{MG} are monotonic, the entropy $S_{\overline{MG}}$ shows a minimum in the vicinity of the dimerization transition. If indeed these are entanglement signatures of this quantum phase transition, it is interesting that it is found in the non-MG part of the state. Of course this part increases in dominance as N increases; see Fig. 3 (top-left plot).

That there is a fairly significant dimerized part that is already present in the small-N Heisenberg model that may be the reason why the entanglement signatures of the transition are not easy to see. But once the dimerized part is excised, at least in part, the remaining "grass" seems to reveal the transition. It should also be noted that calculations not presented show that if the entropy S is itself split into a MG and $\overline{MG}$ part without rescaling the eigenvalues, then these are monotonic on $[0,1/2]$; the interpretation of $S_{\overline{MG}}$ as a entanglement is necessary.

It is also observed that the spectrum of the RDM for various partition sizes $N_A = 2k$ are qualitatively similar including the crossing of the lowest eigenvalue corresponding to the MG subspace with the triplet from the $\overline{MG}$ subspace. The existence of a minimum entropy of entanglement for the $|\psi_{\overline{MG}}(J_2)\rangle$ state between N_A and the rest of the spins is interestingly a robust feature, as shown in Fig. 4. Of course the case $k = 1$ (two-spin RDM) is special, the number of eigenvalues of the

RDM being four and all that remain being nonzero at the MG point. In fact, it is easy to see from the Eq. (6), which becomes a Werner state, that these eigenvalues correspond to the one dominant one and the triplet. The rising state is absent from this spectrum and is a property of chains with more than four spins. It is quite essential that the number of spins in the subsystems A and B are even. If there are an odd number of spins (in the subsystems) the number of eigenvalues in the
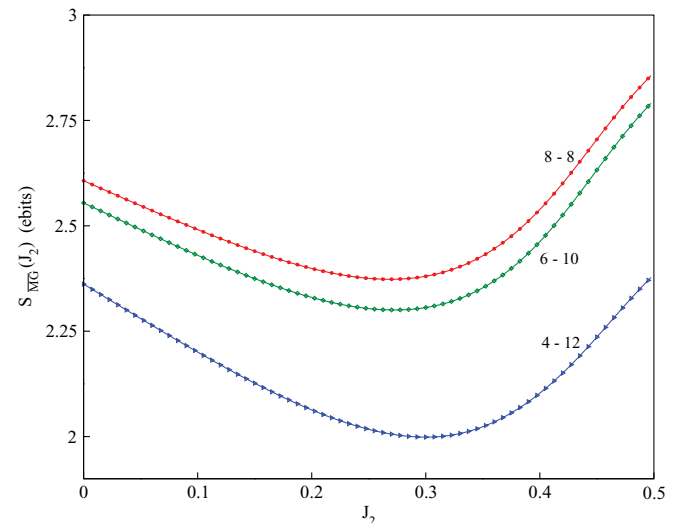

FIG. 4. (Color online) Entropy $S_{\overline{MG}}(J_2)$ for $N = 16$ spins with different bipartition sizes $N_A - N_B$, which are indicated. This is the entanglement of N_A spins with the rest for the $\overline{MG}$ projection. The existence of a minimum is robust to altering partition sizes.

RDM that are nonzero at the MG point is four and the entropy $S_{\overline{MG}}$ remains monotonic in $[0, 1/2]$. There is also the added complication that the ground state of the $J_1 - J_2$ model in this range has zero momentum when $N/2$ is even and momentum π otherwise.

The eigenvalues in $\overline{MG}$ themselves have structure and a hierarchy that is not unlike that of the dimerized state. While the largest triplet $\overline{MG}$ eigenvalue, $\lambda_6(J_2)$ decreases monotonically in $[0, 1/2]$, the scaled value [divided by $\beta^2(J_2)$, see the bottom panel of Fig. 1] shows a single peak again in the vicinity of the dimerization transition, which may be the origin of the minimum in the entropy of the grass. Indeed, $-\log_2[\lambda_6(J_2)/\beta^2(J_2)]$ is the so-called min-entropy, $S_{\infty\overline{MG}}$, and along with the von Neumann entropy is a special case of the Renyi entropies. It is guaranteed from general considerations that $S_{\infty\overline{MG}} < S_{\overline{MG}}$.

To explore entanglement sharing in the pure N-particle states $|\psi_{\overline{MG}}(J_2)\rangle$ and $|\psi_{MG}(J_2)\rangle$ and for a fixed partition $N = N_A + N_B$, one can study multipartite measures and two-spin measures such as concurrence. The latter is studied in the next section, while for the former, the entanglement entropy of m contiguous spins is numerically calculated in the case of symmetric partitions $N_A = N_B$, the results of which are shown in Fig. 5 for a chain of length $N = 16$. The translation symmetry is lost on projection and, by construction, from the Schmidt decomposition, these states have a symmetry of shifting by $N/2$ sites. Thus, it makes a difference as to where the first of the m contiguous spins is chosen. The case of "0 shift" corresponds to the first being also the first in the block of $N/2$ spins that remains after tracing. Further shifts refer to right shifting the first spin in the block by the indicated amount. The rather more complex entanglement sharing of the state $|\psi_{\overline{MG}}(J_2)\rangle$ is seen here. The dependence on the shift of the first spin of the m blocks is clear and for no shift the prominent feature remains the $m = 8$ case that has already been discussed above. However, the case of $m = 4$ also shows a local minimum, albeit a shallow one, in the entanglement at exactly the same value of J_2 as for $m = 8$. The other values of m also indicate the fair amount of multipartite entanglement present in this state. Shifting the first spin away now explores different entanglement features; for instance, with a shift of 1 and $m = 2$, this is the entanglement of spins 2 and 3 with the rest when the whole state is $|\psi_{\overline{MG}}(J_2)\rangle$. The first observation is that there is no minimum anymore for any value of m, especially eight spins. Thus, it is required for the minimum in the entropy that the block coincides with the partitioning in the Schmidt decomposition. The second is the considerably large entanglements that are present; for example, with blocks shifted by three. These are in sharp contrast to the behavior of the corresponding quantities for the state $|\psi_{MG}(J_2)\rangle$, wherein the entanglements are seen to be monotonically increasing and the shifts do not change the features much, and the entanglement entropies are only about half as large.

III. CONCURRENCES IN SCHMIDT VECTORS AND MG, $\overline{MG}$ PROJECTIONS

Attention is now turned to a more detailed study of two-spin entanglements. In particular, one wishes to know the nature of entanglement in the eigenstates of the RDM of ρ_{N_A}.

These correspond to the N_A-particle Schmidt vectors in a Schmidt decomposition of the ground state. Also of interest is the concurrences present in the corresponding projected N-particle pure states $|\psi_{MG}\rangle$ and $|\psi_{\overline{MG}}\rangle$. The concurrence is a one-to-one function of the entanglement of formation and the recipe to obtain the concurrence between any pair of spins which are either in a pure or a mixed state ρ is as follows [26]: Compute the eigenvalues of the matrix $\rho(\sigma^y \otimes \sigma^y)\rho^*(\sigma^y \otimes \sigma^y)$ (the complex conjugation being done in the computational basis). The eigenvalues are guaranteed to be positive and if they are arranged as $\{\lambda_1 \geqslant \lambda_2 \geqslant \lambda_3 \geqslant \lambda_4\}$, the concurrence between the pair of spins considered is given by $C = \max[0, \sqrt{\lambda_1} - \sqrt{\lambda_2} - \sqrt{\lambda_3} - \sqrt{\lambda_4}]$. The concurrence C is such that $0 \leqslant C \leqslant 1$, with zero for the case of an unentangled state and unity when it is maximally entangled.

Recall that the MG subspace for a given even partition is spanned by five states whose corresponding eigenvalues are a large and decreasing one, three degenerate and nearly constant ones, while the last is small and increasing. Concentrating on the case $N_A = N/2$ and N an even integer, it is sufficient to study the $N/2$-particle pure states $|\phi_1(J_2)\rangle_A$, $|\phi_{2,3,4}(J_2)\rangle_A$, and $|\phi_5(J_2)\rangle_A$ [see Eq. (9)], respectively. Collectively they contribute to the normalized state $|\psi_{MG}(J_2)\rangle$. The complementary subspace is the normalized state $|\psi_{\overline{MG}}(J_2)\rangle$ whose principal contribution comes from a triplet whose eigenvalue is decreasing and intersects with the increasing lowest eigenvalue from the MG subspace. In all of these states one can look at the nature of pairwise entanglement via nearest-neighbor pairwise concurrence [26], which is a genuine and well-used measure of entanglement between two qubits or spin-$\frac{1}{2}$ particles, especially useful when they are not in a pure state. One may study the concurrences $C_{(i,i+1)}(J_2)$ between spin at i and $i + 1$ (identifying $L + 1$ as the first spin), as well as their totals either over the entire chain, or over two parts, where i is even or when it is odd. Note that while the ground state has translational invariance, this is typically broken in the states $|\psi_{MG}(J_2)\rangle$ and $|\psi_{\overline{MG}}(J_2)\rangle$ and the corresponding Schmidt vectors. Thus, $C_{(i,i+1)}(J_2)$ are typically different for different values of i, unlike in the original state.

As the dimer part of the state survives until the MG point, it is likely to have large pairwise concurrences. The top panel of Fig. 6 shows these for the most dominant state; namely, $|\phi_1(J_2)\rangle_A$ and the rising state $|\phi_5(J_2)\rangle_A$. It is seen that the nearest-neighbor concurrences show a clear progress to dimerization as J_2 increases. In the case of $|\phi_1(J_2)\rangle_A$, the entanglement between the alternate bonds starting from the first is large and increases with J_2, while the others decrease and vanish well before the MG point, and in this respect are like $|R_{N/2}\rangle$; for $|\phi_5(J_2)\rangle_A$ the highly entangled bonds start from the second spin, and in this respect are like $|L_{N/2}\rangle$. The insets show the sum of the concurrences in the even and odd sublattices of the $N/2$ spin chain, and it is seen that the entanglements vanish in the alternate bonds again in the vicinity of the dimerization transition, but not at exactly one point. Also notice that for $|\phi_5(J_2)\rangle_A$ entanglement develops for distant spins at sites 1 and 8 for the case shown of $N = 16$. The full chain has been "cut" keeping sites 1–8 and tracing out 9–16. This singles out the sites 1 and 8; also note the reflection symmetry that is apparent from the distribution of concurrences amongst spins 1–8. It may be noted that the
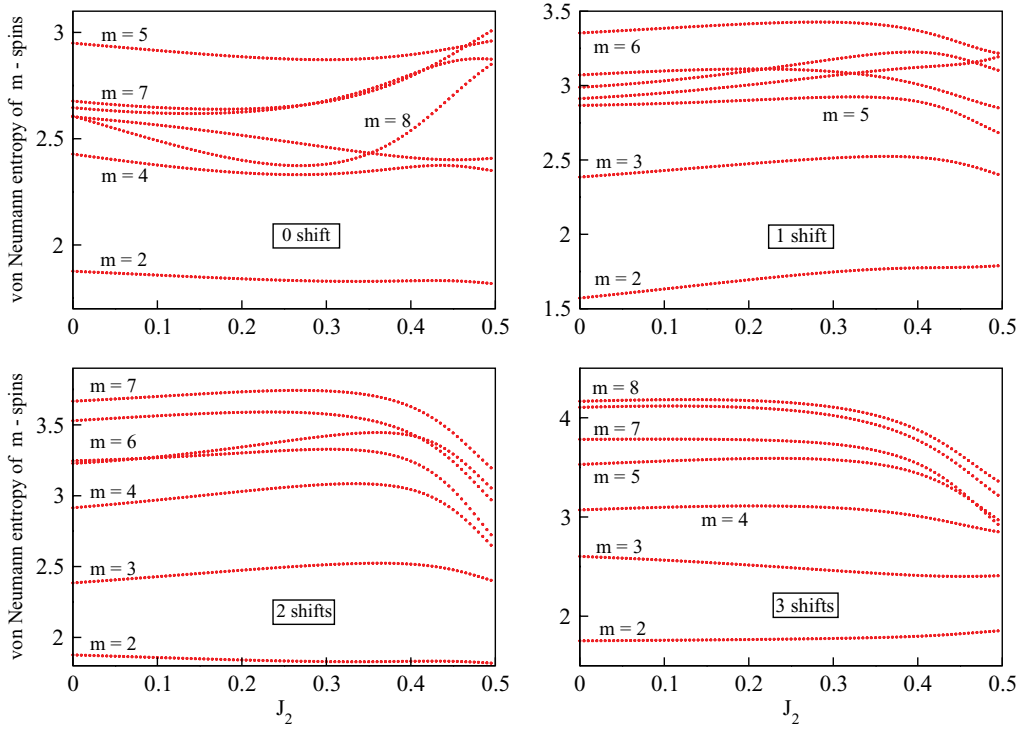
FIG. 5. (Color online) Entanglement entropy between m contiguous spins and the rest for state $|\psi_{\overline{MG}}\rangle$. Here $N = 16$, and "shift" refers to the first spin site in the block of m spins.

concurrences for the case of the ground state do not show such structures that reveal the dimerization [15,28,29].

In case of the triplets (as in the MG subspace, or the states corresponding to the largest eigenvalue in the $\overline{MG}$ subspace) the states are not unique due to degeneracy. However, the projector onto the degenerate three-dimensional subspace is unique and can be used to define a density matrix. For example, for the triplet in the MG subspace consider the state

$$\rho_{234}(J_2) = \tfrac{1}{3}[|\phi_2(J_2)\rangle_{AA}\langle\phi_2(J_2)| + |\phi_3(J_2)\rangle_{AA}\langle\phi_3(J_2)| + |\phi_4(J_2)\rangle_{AA}\langle\phi_4(J_2)|], \quad (11)$$

and the corresponding mixed state for the most prominent triple of $\overline{MG}$, say ρ_{678}. The concurrence in the bonds of these states are shown in the lower panel of Fig. 6. The state ρ_{234} displays large entanglements in the alternative bonds starting from the second spin and is in this respect like the rising state $|\phi_5(J_2)\rangle$, except that there is here no entanglement between the distant spins 1 and 8. This distinction from the rising state is understood upon calculating the two-qubit reduced density matrix of the triplet density matrix at $J_2 = 1/2$:

$$(\rho_{234}(J_2 = 1/2))_{18} = \tfrac{1}{3}(|00\rangle\langle00| + |11\rangle\langle11| + |++\rangle\langle++|). \quad (12)$$

The reduced density matrix of spins 1 and 8 is $(\rho_{234}(J_2 = 1/2))_{18}$; the state $|+\rangle = (|0\rangle + |1\rangle)/\sqrt{2}$. The separability of these spins in this density matrix is then evident, and entanglement appears to be absent not only at $J_2 = 1/2$ but for the entire range considered. The entanglement of other bonds decrease from the Heisenberg point and vanish again well before the MG point. Indeed the point where the dimer

states takes on a pure alternate bond entanglement is again in the region of the dimerization transition.

A similar analysis for ρ_{678} is shown in the same figure and presents a somewhat different picture, with the dimerization not being uniformly present. While the concurrence between 3-4 and the symmetric 5-6 spins are large, the rest of the nearest-neighbor entanglements are nearly zero. The concurrences that is present in the 3-4 pair is also decreasing from the Heisenberg chain as the MG point is approached. It is observed that the entanglement between the 1-2 and 7-8 pairs, which starts at zero, develops as J_2 increases and is nonzero at $J_2 = 1/2$. This indicates the existence of some dimerization in the $\overline{MG}$ subspace, but of a different kind than in the MG subspace. The effective overall decrease of the two-qubit entanglements is in sharp contrast to that found for the Schmidt vectors that span the MG subspace.

To analyze this further, pair concurrences were calculated for the N-spin state $|\psi_{\overline{MG}}(J_2)\rangle$ and the nearest-neighbor pair concurrence is shown in the left part of Fig. 7. While this looks similar to the case of the state ρ_{678}, which is indeed the dominant part of $|\psi_{\overline{MG}}(J_2)\rangle$, the prominent difference is the somewhat large entanglement between the 1-16 and 8-9 pairs (here $N = 16$) which exists for the Heisenberg chain and which decreases away as the MG point is approached. Once again the overall decrease in the concurrence is in contrast to that for the Schmidt vectors in the MG subspace and is consistent with an increase of the von Neumann entropy in as much as one can think of monogamy of entanglement being operative and the entanglement becomes of a more multipartite kind. Indeed, the structure of even the two-spin entanglements present in this state is neither of an $|L_N\rangle$ kind nor of a $|R_N\rangle$ kind, but rather a mixture with some bonds being either very
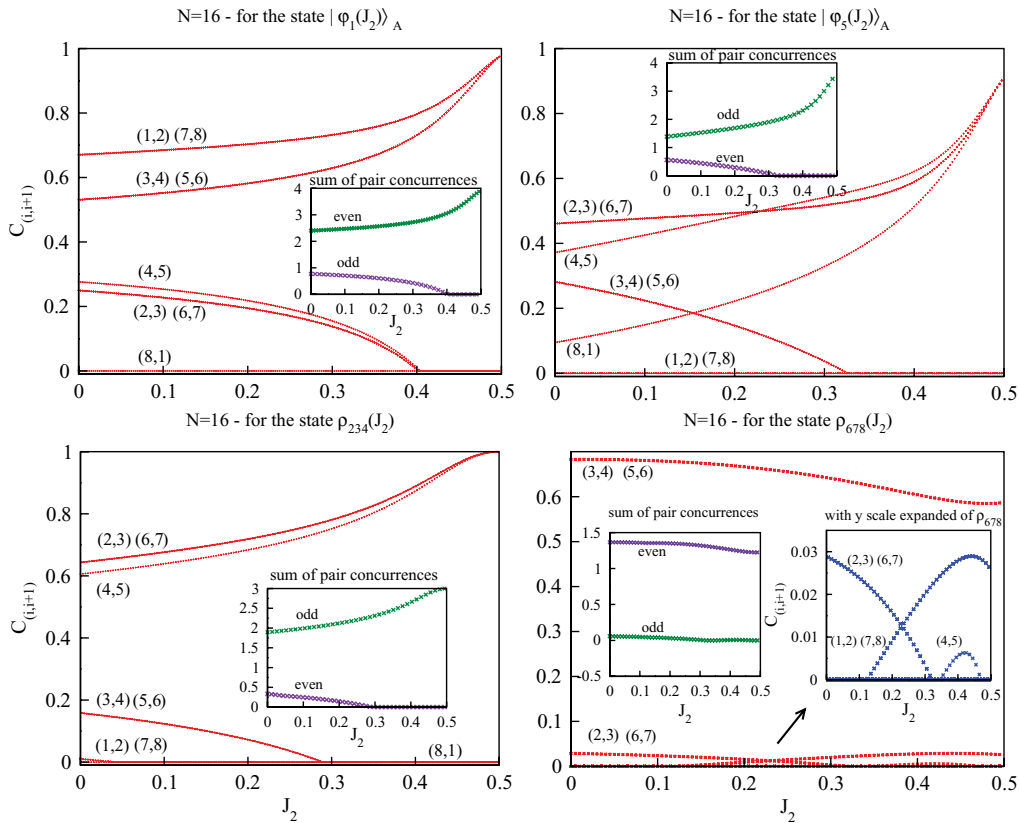
FIG. 6. (Color online) Concurrence between neighboring spins in Schmidt vectors, which are pure states of $N/2$ spins, for symmetric-partition case of $N = 16$. The top left is for the vector $|\phi_1(J_2)\rangle$ corresponding to the highest eigenvalue, top right is for the vector $|\phi_5(J_2)\rangle$ corresponding to the rising eigenvalue, while the bottom left is for the mixed state ρ_{234} corresponding to the triplet. The bottom right plot is for the mixed state ρ_{678} corresponding to the largest triplet of eigenvalues corresponding to states in the $\overline{MG}$ subspace. The insets in the corresponding graphs show the sum of the alternate pair concurrences for each of the above-described eigenstates.

weakly or not at all entangled. For example, the entanglement present in 1-16 and 8-9 is consistent with an $|L_N\rangle$ kind of dimerization, while the prominent entanglement between 3-4 and 5-6 resembles $|R_N\rangle$. It is interesting that, as the

dimerization progresses, even in this grass contribution there is a tendency to choose a type of dimerization, with the $|L_N\rangle$ kind taking a back seat at around the dimerization transition. However, the decrease in the concurrence is also consistent
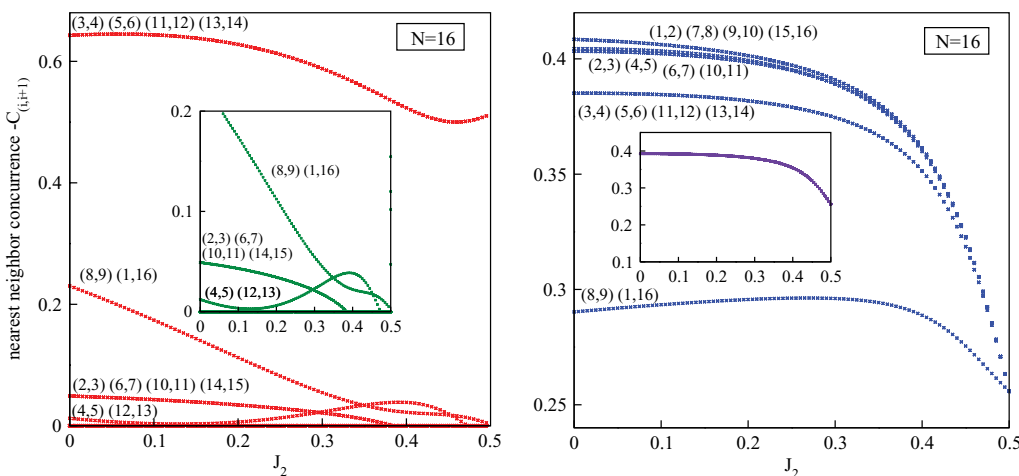

FIG. 7. (Color online) Left panel shows nearest-neighbor concurrence in $N = 16$ spin state $|\psi_{\overline{MG}}(J_2)\rangle$. The spin pairs are indicated above their corresponding curves and the inset is a magnification of the y axis. The pairs not indicated [namely $(1,2)$, $(7,8)$, $(9,10)$, $(15,16)$], have zero concurrence throughout. Right panel shows nearest-neighbor concurrence in $N = 16$ spin state $|\psi_{MG}(J_2)\rangle$ and in translationally symmetric ground state $|\Psi(J_2)\rangle$ (inset).

with a rising entropy, as observed in Fig. 3 (bottom right). The principal features discussed above have been verified to remain intact for the case of $N = 24$ spins.

To contrast the nearest-neighbor entanglement of the more complicated state $|\psi_{\overline{MG}}(J_2)\rangle$ with those in $|\psi_{MG}(J_2)\rangle$ and in the original translation symmetric ground state $|\Psi(J_2)\rangle$, the latter two quantities are plotted in the right part of Fig. 7. The broken translation symmetry in $|\psi_{MG}(J_2)\rangle$ implies that there is more than one NN concurrence value; however, as indicated earlier there persists a symmetry of translation by $N/2$ sites as well reflection symmetry. Together they indicate that five different nearest-neighbor concurrence values are possible for a chain of $N = 16$ spins and these are shown along with the bond labels in Fig. 7. The low value of the entanglement where the bonds are cut (8-9 and 1-16) compared to the others may be noted. In contrast, that $|\psi_{\overline{MG}}(J_2)\rangle$ displays much lesser concurrence is also clear. The original translation symmetric state has one NN concurrence that decreases towards the MG point where it reaches a value close to 1/4 (which is achieved for $N = \infty$ [27]). Interestingly, its value is slightly smaller than that for the $|\psi_{MG}(J_2)\rangle$ subspace and may be due to the mixing of the state's $\overline{MG}$ projection.

IV. DISCUSSIONS AND SUMMARY

In this paper the frustrated $J_1 - J_2$ antiferromagnetic Majumdar-Ghosh model has been revisited with a view on entanglement properties, both multipartite and those between pairs of spins. Entanglement studies of the ground state that have revealed signatures of the dimerization transition have hitherto relied on scaling of the entropy with the system size. However, in this paper several suggestive simple signatures are presented, from those that involve von Neumann entropy to concurrence between spins. For this the principal tool is the well-known Schmidt decomposition that combined with the existence of the unique MG point ($J_2/J_1 = 1/2$) provided an opportunity for a projection of the ground state into two orthogonal subspaces that are unique once the partition in the Schmidt decomposition is fixed. The dominant subspace is only five dimensional and contains the complete state at the MG point. The complementary subspace whose significance wanes from the Heisenberg point ($J_2/J_1 = 0$) contributes only marginally, but this contribution increases with the number of spins N; for instance for $N = 16$ this contribution is roughly 3% when $J_2/J_1 = 0$. These subspaces are indicated as MG and $\overline{MG}$, although again the partition dependence in the Schmidt decomposition is implicit.

The entanglement between N_A spins and the rest of the spin chain is known to have different scaling laws as criticality is lost at $J_2/J_1 \approx 0.24$. What is shown above is that while the entanglement of the full or dominant projection in the MG subspace is monotonic, the projection onto $\overline{MG}$ has a minimum in the vicinity of the transition for even N_A, at least for the values of N that have been explored. This feature is robust against various different partitions of the ground state. How robust this feature is to increasing number of spins remains to be seen.

To understand better the behavior of entropies, one may calculate further the entanglements present after the states $|L_N\rangle$ or $|R_N\rangle$ are projected out from the ground state $|\Psi(J_2)\rangle$. That
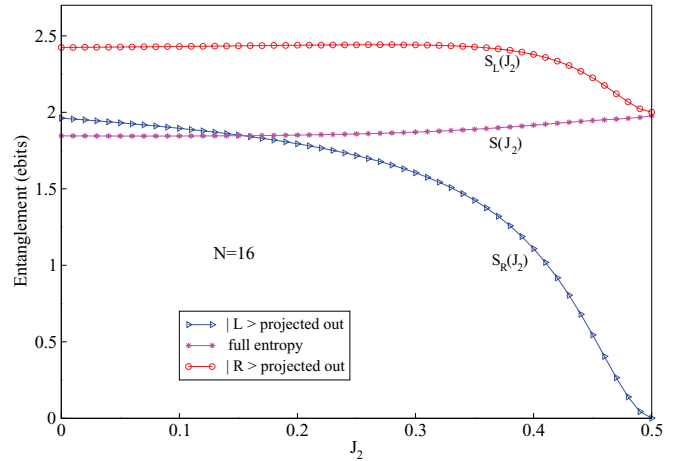

FIG. 8. (Color online) Entanglements of half the chain with the rest for $S_R(J_2)$ and $S_L(J_2)$ after projecting out fully dimerized $|L_N\rangle$ or $|R_N\rangle$ states, respectively. Shown also is the case for the complete ground-state entanglement $S(J_2)$ for comparison, and here $N = 16$ spins are used.

is the quantities $S_L(J_2) = S([|\Psi(J_2)\rangle - |R_N\rangle\langle R_N|\Psi(J_2)\rangle]t)$ and $S_R(J_2) = S([|\Psi(J_2)\rangle - |L_N\rangle\langle L_N|\Psi(J_2)\rangle]t)$, the entanglements of $N/2$ contiguous spins with the rest (t is a normalization constant) are found and plotted in Fig. 8. Note that $S_L(J_2)$ tends to the entanglement of the state $|L_N\rangle$ at the MG point (i.e., 2), while $S_R(J_2)$ tends to that of $|R_N\rangle$ (i.e., 0). It is interesting to note that the entanglement of these symmetry-broken states are now monotonically decreasing already for small values of N, reflecting well the fact that the entanglement sharing in the spins is changing from a more complex situation at the Heisenberg point to the fully dimerized situation at the MG point. The dimerization, which is leading to the formation of couples that are unentangled with any other spin, discourages multipartite entanglement.

An important complementary view of entanglement sharing is provided by calculating the concurrence between pairs of spins. The state in which these are measured are, however, not the ground state itself, but the eigenfunctions of the reduced density matrix, or the Schmidt vectors. The Schmidt vectors (now pure states of N_A spins) of the MG subspace show a clear progress towards dimerization as J_2 increases with the most dominant state resembling $|R_{N/2}\rangle$ and the rising state $|L_{N/2}\rangle$. The triplet also shows dimerization as in $|L_{N/2}\rangle$ except for the end spins being unentangled. Here "dimerization" is seen as the vanishing of concurrence on a sublattice, while the complementary one develops into pairs with maximum concurrence. The most dominant eigenvalue corresponding to triply degenerate states in the $\overline{MG}$ subspace was also studied using pair concurrences and it presents a different picture compared to the five Schmidt vectors in the MG subspace, in that the concurrences tend to decrease as the MG point is approached. The projection of the state on the N-particle $\overline{MG}$ subspace, $|\psi_{\overline{MG}}(J_2)\rangle$, also shows interesting differences and larger multipartite entanglements. The initial decrease of the entropy $S_{\overline{MG}}$ which contributes to the nonmonotonic character of this entropy may have its origins in the overall tendency for decreasing entropy as evidenced by projecting out the $|L_N\rangle$

or $|R_N\rangle$ states; however, more study is warranted on the exact origins and significance, if any, of this.

If a bipartite split with one block containing the spins at odd sites and the other block containing the spins at even sites ("comb entanglement") is taken, it presents a complex entanglement spectrum with many crossings, and while this is interesting, the dimerization transition seems difficult to unravel. Also, the present study has calculated non-nearest-neighbor concurrence in the various states presented, but most of them are indeed zero. Preliminary investigations of the $J_1 - J_2$ model with quenched disorder in J_2 reveals a certain robustness of the above analysis. Small disorders lead to the exact crossing at the MG point being replaced by an avoided one, and there is still to a large extent only a five-dimensional dominant space and hence a split into a MG and $\overline{MG}$ subspaces persists. Further study is needed on how nondimerized subspaces such as $\overline{MG}$ dominate in the large-N limit.

While this work has concentrated on the range $0 \leqslant J_2 \leqslant 1/2$, it is naturally interesting to look beyond this range. The crossing of the first excited state with momentum π at $J_2 = 1/2$ with the zero-momentum ground state is followed for small N (such as used here) with several other intersections between the same two states for $J_2 > 1/2$. This rather complex phase is interesting, and especially so when the methodology of this paper is applied to it, and is currently under investigation.

APPENDIX: COMPUTATION OF REDUCED DENSITY MATRIX AND ITS SPECTRUM AT MG POINT

There is more than one way to derive the reduced density matrix, and in the following a direct approach is used. First start with the superposition $|\psi\rangle = \alpha_1|R_N\rangle + \alpha_2|L_N\rangle$ of the two dimer states that are eigenfunctions at the MG point; namely $|R_N\rangle$ and $|L_N\rangle$ [as given in Eq. (2)].

Let the bipartite split consist of (i) block A with $2k$ contiguous spins and (ii) block B with the rest. One traces over block B to find the reduced density matrix:

$$\rho_{2k} = \text{tr}_B(|\psi\rangle\langle\psi|) = \alpha_1^2 \rho_{2k_1} + \alpha_2^2 \rho_{2k_2} + \alpha_1\alpha_2(\rho_{2k_3} + \rho_{2k_3}^\dagger),$$
(A1)

where $\rho_{2k_1} = \text{tr}_B(|R_N\rangle\langle R_N|)$, $\rho_{2k_2} = \text{tr}_B(|L_N\rangle\langle L_N|)$, and $\rho_{2k_3} = \text{tr}_B(|R_N\rangle\langle L_N|)$.

Denote now $|R_{2k}\rangle \equiv (12)(34)\cdots(2k-1\,2k)$ and $|L_{2k-2}\rangle \equiv (23)(45)\cdots(2k-2\,2k-1)$; these being spin states which are not affected by the partial tracing operation. It is straightforward to calculate ρ_{2k_1} because no singlet "bonds" are cut due to the structure of $|R_N\rangle$. However, for calculating ρ_{2k_2} the singlets between $(N1)$ and $(2k\,2k+1)$ are broken, which results in maximally mixed states $\frac{I_1}{2}$ and $\frac{I_{2k}}{2}$ at the ends. The remaining tensor products of singlets $|L_{2k-2}\rangle$ are left unaffected. Thus it

follows that

$$\rho_{2k_1} = \alpha_1^2|R_{2k}\rangle\langle R_{2k}|,$$
$$\rho_{2k_2} = \frac{\alpha_2^2}{4}\left(I_1 \otimes |L_{2k-2}\rangle\langle L_{2k-2}| \otimes I_{2k}\right).$$
(A2)

The remaining part involves cross terms, which is written explicitly by introducing standard σ_z basis for the spins in block B:

$$\rho_{2k_3} = \sum_{i_{2k+1},\ldots,i_N\in\{0,1\}} \langle i_{2k+1}\cdots i_N|R_N\rangle\langle L_N|i_{2k+1}\cdots i_N\rangle. \quad \text{(A3)}$$

It is easy to verify that $\langle i_1 i_2|(|01\rangle - |10\rangle) = (-1)^i\delta_{i_1,i_2\oplus 1}$, where the $\oplus$ denotes an addition modulo 2. The expression

$$\langle i_{2k+1}i_{2k+2}\cdots i_N|R_N\rangle$$
$$= \frac{(-1)^{i_{2k+1}+i_{2k+3}+\cdots+i_{N-1}}}{(\sqrt{2})^{(N-2k)/2}}\delta_{i_{2k+1},i_{2k+2}\oplus 1}\cdots\delta_{i_{N-1},i_N\oplus 1}|R_{2k}\rangle \quad \text{(A4)}$$

and a similar expression are found for $\langle L_N|i_{2k+1}i_{2k+2}\cdots i_N\rangle$, which involves the untraced part $|L_{2k-2}\rangle$ as follows:

$$\langle L_N|i_{2k+1}i_{2k+2}\cdots i_N\rangle$$
$$= \langle L_{2k-2}|\left(\frac{1}{\sqrt{2}}\right)^{[(N-2k)/2]-2}\delta_{i_{2k+2}i_{2k+3}\oplus 1}\cdots\delta_{i_{N-2}i_{N-1}\oplus 1}$$
$$\times \langle(2k\,2k+1)|i_{2k+1}\rangle\langle(N1)|i_N\rangle \quad \text{(A5)}$$

The "end spins" are taken into account as $\langle(2k\,2k+1)|i_{2k+1}\rangle = \frac{1}{\sqrt{2}}(\langle 0|_{2k}\delta_{1,i_{2k+1}} - \langle 1|_{2k}\delta_{0,i_{2k+1}})$ and $\langle(N1)|i_N\rangle = \frac{1}{\sqrt{2}}(\langle 1|_1\delta_{0,i_N} - \langle 0|_1\delta_{1,i_N})$. Using this expression along with Eqs. (A4) and (A5) and substituting them in Eq. (A3), the final form of ρ_{2k} (after some straightforward algebra taking care of the modulo 2 addition) is found to be

$$\rho_{2k} = \alpha_1^2|R_{2k}\rangle\langle R_{2k}| + \alpha_2^2\left[\frac{I_1}{2} \otimes |L_{2k-2}\rangle\langle L_{2k-2}| \otimes \frac{I_{2k}}{2}\right]$$
$$+ \frac{\alpha_1\alpha_2}{2^{(N-2k)/2}}(-1)^{(N-2k)/2}\left[|R_{2k}\rangle\langle L_{2k}| + |L_{2k}\rangle\langle R_{2k}|\right].$$
(A6)

It is to be noted from the structure of ρ_{2k} that the coherent term is only of the order of $2^{-(N-2k)/2}$ and hence exponentially decreases with the number of spins in block B.

The eigenvalues of ρ_{2k} are now calculated. For notational convenience, for K spins, we define

$$p = \langle R_K|L_K\rangle = (-1)^{K/2}2^{(1-K/2)},$$
$$\gamma = \frac{\alpha_1\alpha_2(-1)^{(N-2k)/2}}{2^{(N-2k)/2}}.$$

Writing the $I_1 \otimes I_{2k}$ in $(I_1 \otimes |L_{2k-2}\rangle\langle L_{2k-2}| \otimes I_{2k})$ as the sum of projectors into the four-Bell basis, $|\phi_b^l\rangle$ ($1 \leqslant l \leqslant 4$) we can define new states $|L_{2k}^l\rangle = |L_{2k-2}\rangle \otimes |\phi_b^l\rangle_{2k,1}$; here $l = 1, 2, 3, 4$, we then use the (easily obtained) properties that $\langle R_{2k}|L_{2k}^l\rangle = \langle L_{2k}|L_{2k}^l\rangle = 0$; $l = 1, 2, 3$. Explicitly,

$$|L_{2k}^1\rangle = |L_{2k-2}\rangle[(|01\rangle + |10\rangle)/\sqrt{2}]_{2k,1},$$
$$|L_{2k}^2\rangle = |L_{2k-2}\rangle[(|00\rangle + |11\rangle)/\sqrt{2}]_{2k,1},$$
$$|L_{2k}^3\rangle = |L_{2k-2}\rangle[(|00\rangle - |11\rangle)/\sqrt{2}]_{2k,1},$$
$$|L_{2k}^4\rangle = |L_{2k-2}\rangle[(|01\rangle - |10\rangle)/\sqrt{2}]_{2k,1} = |L_{2k}\rangle.$$

Now using the above we can rewrite ρ_{2k} as

$$\rho_{2k} = \alpha_1^2 |R_{2k}\rangle\langle R_{2k}| + \frac{\alpha_2^2}{4}|L_{2k}\rangle\langle L_{2k}| + \frac{\alpha_2^2}{4}\left[\sum_{l=1}^{3}|L_{2k}^l\rangle\langle L_{2k}^l|\right]$$
$$+ \gamma\left[|R_{2k}\rangle\langle L_{2k}| + |L_{2k}\rangle\langle R_{2k}|\right]. \tag{A7}$$

It is straightforward to verify that $|L_{2k}^1\rangle$, $|L_{2k}^2\rangle$, and $|L_{2k}^3\rangle$ are three eigenstates of ρ_{2k} with degenerate eigenvalues $\alpha_2^2/4$. This corresponds to the triply degenerate eigenvalue in the entanglement spectrum at the MG point. It is clear that the other eigenvalues correspond to eigenvectors in the two-dimensional subspace spanned by $|R_{2k}\rangle$ and $|L_{2k}\rangle$, and hence there are only two of these. Either defining the orthogonal vectors $|R_{2k}\rangle \pm |L_{2k}\rangle$ or proceeding to define linear superpositions of $|R_{2k}\rangle$ and $|L_{2k}\rangle$ as the eigenvectors, a straightforward (if somewhat lengthy) calculation leads to Eq. (8). These two eigenvalues correspond to the most dominant state and the rising state in the entanglement spectrum of ρ_{2k}.

[1] L. Amico, R. Fazio, A. Osterloh, and V. Vedral, Rev. Mod. Phys. **80**, 517 (2008).

[2] J. Zhang, T.-C. Wei, and R. Laflamme, Phys. Rev. Lett. **107**, 010501 (2011).

[3] G. Vidal, J. I. Latorre, E. Rico, and A. Kitaev, Phys. Rev. Lett. **90**, 227902 (2003).

[4] A. Chandran, D. Kaszlikowski, A. Sen(De), U. Sen, and V. Vedral, Phys. Rev. Lett. **99**, 170502 (2007).

[5] D. Kaszlikowski, W. Son, and V. Vedral, Phys. Rev. A **76**, 054302 (2007).

[6] J. I. Latorre and A. Riera, J. Phys. A: Math. Theor. **42**, 504002 (2009).

[7] R. Horodecki, P. Horodecki, M. Horodecki, and K. Horodecki, Rev. Mod. Phys. **81**, 865 (2009).

[8] D. P. DiVincenzo, Proc. R. Soc. London, Ser. A **454**, 261 (1998).

[9] C. H. Bennett and P. W. Shor, Science **284**, 747 (1999).

[10] C. H. Bennett, D. P. DiVincenzo, J. A. Smolin, and W. K. Wootters, Phys. Rev. A **54**, 3824 (1996).

[11] C. H. Bennett, G. Brassard, C. Crépeau, R. Jozsa, A. Peres, and W. K. Wootters, Phys. Rev. Lett. **70**, 1895 (1993).

[12] S. Sachdev, *Quantum Phase Transitions* (Cambridge University Press, New York, 2011).

[13] T. J. Osborne and M. A. Nielsen, Phys. Rev. A **66**, 032110 (2002).

[14] A. Osterloh, L. Amico, G. Falci, and R. Fazio, Nature (London) **416**, 608 (2002).

[15] X.-F. Qian, T. Shi, Y. Li, Z. Song, and C. P. Sun, Phys. Rev. A **72**, 012333 (2005).

[16] L. A. Wu, M. S. Sarandy, and D. A. Lidar, Phys. Rev. Lett. **93**, 250404 (2004).

[17] V. Alba, L. Tagliacozzo, and P. Calabrese, Phys. Rev. B **81**, 060411(R) (2010).

[18] C. Holzhey, F. Larsen, and F. Wilczek, Nucl. Phys. B **424**, 443 (1994).

[19] P. Calabrese and J. Cardy, J. Stat. Mech. (2004) P06002.

[20] F. Alet, I. P. McCulloch, S. Capponi, and M. Mambrini, Phys. Rev. B **82**, 094452 (2010).

[21] Y.-C. Lin and A. W. Sandvik, Phys. Rev. B **82**, 224414 (2010).

[22] P. Facchi, G. Florio, C. Invernizzi, and S. Pascazio, Phys. Rev. A **78**, 052302 (2008).

[23] G.-H. Liu, C.-H. Wang, and X.-Y. Deng, Phys. B (Amsterdam, Neth.) **406**, 100 (2011).

[24] R. W. Chhajlany, P. Tomczak, and A. Wójcik, Phys. Rev. Lett. **99**, 167204 (2007).

[25] P. Sadhukhan and S. M. Bhattacharjee, J. Phys. A: Math. Theor. **45**, 425302 (2012).

[26] W. K. Wootters, Phys. Rev. Lett. **80**, 2245 (1998).

[27] S.-J. Gu, H. Li, Y.-Q. Li, and H.-Q. Lin, Phys. Rev. A **70**, 052302 (2004).

[28] L. C. Kwek, Y. Takahashi, and K. W. Choo, J. Phys: Conf. Ser. **143**, 012014 (2009).

[29] S. Zhe, W. Xiao-Guang, H. An-Zi, and L. You-Quan, Commun. Theor. Phys. **43**, 1033 (2004).

[30] R. Eryiğit, Int. J. Theor. Phys. **48**, 885 (2009).

[31] C. K. Majumdar and D. K. Ghosh, J. Math. Phys. **10**, 1388 (1969).

[32] C. K. Majumdar and D. K. Ghosh, J. Math. Phys. **10**, 1399 (1969).

[33] K. Okamoto and K. Nomura, Phys. Lett. A **169**, 433 (1992).

[34] R. Chitra, S. Pati, H. R. Krishnamurthy, D. Sen, and S. Ramasesha, Phys. Rev. B **52**, 6581 (1995).

[35] F. Alet, S. Capponi, N. Laflorencie, and M. Mambrini, Phys. Rev. Lett. **99**, 117204 (2007).

[36] R. W. Chhajlany, P. Tomczak, A. Wójcik, and J. Richter, Phys. Rev. A **75**, 032340 (2007).

[37] A. Sen(De) and U. Sen, arXiv:1002.1253 [quant-ph].

[38] P. M. van den Broek, J. Phys. C: Solid State Phys. **13**, 5423 (1980).

[39] A. W. Sandvik, AIP Conf. Proc. **1297**, 135 (2010).

[40] H. A. Bethe, Z. Physik **71**, 205 (1931).

[41] H. Li and F. D. M. Haldane, Phys. Rev. Lett. **101**, 010504 (2008).

[42] D. Poilblanc, Phys. Rev. Lett. **105**, 077202 (2010).

[43] P. Calabrese and A. Lefevre, Phys. Rev. A **78**, 032329 (2008).

[44] K. S. D. Beach and A. Sandvik, Nucl. Phys. B **750**, 142 (2006).

[45] H. Fan, V. Korepin, and V. Roychowdhury, Phys. Rev. Lett. **93**, 227203 (2004).

[46] H. Katsura, N. Kawashima, A. N. Kirillov, V. E. Korepin, and S. Tanaka, J. Phys. A: Math. Theor. **43**, 255303 (2010).

[47] S. Capponi, F. Alet, and M. Mambrini, Mod. Phys. Lett. B **25**, 917 (2011).